Smooth Termination of Rotational Bands in ^{62}Zn: Evidence for a Loss of Collectivity

C. E. Svensson,[1] C. Baktash,[2] G. C. Ball,[3] J. A. Cameron,[1] M. Devlin,[4] J. Eberth,[5] S. Flibotte,[1] A. Galindo-Uribarri,[3,*] D. S. Haslip,[1] V. P. Janzen,[3] D. R. LaFosse,[4] I. Y. Lee,[6] A. O. Macchiavelli,[6] R. W. MacLeod,[6] J. M. Nieminen,[1] S. D. Paul,[2] D. C. Radford,[3,†] L. L. Riedinger,[7] D. Rudolph,[8] D. G. Sarantites,[4] H. G. Thomas,[5] J. C. Waddington,[1] D. Ward,[3,†] W. Weintraub,[7] J. N. Wilson,[1] A. V. Afanasjev,[9,‡] and I. Ragnarsson[9]

[1]*Department of Physics and Astronomy, McMaster University, Hamilton, Ontario, Canada L8S 4M1*

[2]*Physics Division, Oak Ridge National Laboratory, Oak Ridge, Tennessee 37831-6371*

[3]*Atomic Energy of Canada Limited, Chalk River Laboratories, Chalk River, Ontario, Canada K0J 1J0*

[4]*Chemistry Department, Washington University, St. Louis, Missouri 63130*

[5]*Institut für Kernphysik, Universität zu Köln, D-50937 Köln, Germany*

[6]*Nuclear Science Division, Lawrence Berkeley Laboratory, Berkeley, California 94720*

[7]*Department of Physics and Astronomy, University of Tennessee, Knoxville, Tennessee 37996*

[8]*Sektion Physik, Ludwig-Maximilians-Universität München, D-85748 Garching, Germany*

[9]*Department of Mathematical Physics, Lund Institute of Technology, S-22100 Lund, Sweden*

(Received 8 September 1997)

Two sets of strongly coupled rotational bands have been identified in ^{62}Zn. These bands have been observed up to the terminating states of their respective configurations. Lifetime measurements indicate that the transition quadrupole moments in these bands decrease as termination is approached. These results establish the first terminating states of rotational bands in the $A \sim 60$ mass region and confirm the predicted loss of collectivity associated with smooth band termination. [S0031-9007(98)05590-2]

PACS numbers: 21.10.Re, 21.10.Ky, 23.20.Lv, 27.50.+e

In recent years it has become possible to observe rotational bands in heavy nuclei which gradually exhaust the angular momentum content of their single-particle configurations. Such bands were first predicted and observed in nuclei around ^{158}Er [1]. More recently, rotational bands which either reach or approach their terminating states have been observed over extended spin ranges in ^{109}Sb [2,3] and neighboring nuclei [4], and bands approaching termination have been identified in a few $A \sim 80$ nuclei [5] and one $A \sim 60$ nucleus [6]. These smoothly terminating bands are predicted to show a continuous transition from states of high collectivity at intermediate spins to a pure particle-hole (noncollective) state of maximum spin in which the angular momenta of all valence particles and holes are quantized along one axis. Such bands provide a unique opportunity to study the interplay between collective and single-particle degrees of freedom within a single nuclear configuration, and studies of these bands in $A \sim 60$ nuclei are of particular interest because the limited number of particles in these nuclei will enable comparisons between the mean-field cranking models traditionally used for heavy nuclei and the results of large-scale shell model calculations which should soon be possible in this mass region [7]. Although transition quadrupole moment measurements up to termination would provide a crucial test of the predicted loss of collectivity inherent in the present interpretation of smoothly terminating bands, such measurements have not been possible to date. In this Letter we report the first observation of terminating states of rotational bands in the $A \sim 60$ mass region and present evidence from quadrupole moment measurements indicating that these bands do indeed lose collectivity as they approach termination.

High-spin states in ^{62}Zn were populated via the ^{40}Ca(^{28}Si, $\alpha 2p$)^{62}Zn reaction in two experiments with thin ($\sim$0.5 mg/cm^2) self-supporting targets. A 115-MeV ^{28}Si beam was first used and 1.8×10^8 particle-γ-γ coincidence events were detected with the Miniball [8], a 44-element CsI(Tl) charged-particle detector array, and the 8π γ-ray spectrometer [9] comprising 20 Compton-suppressed Ge detectors and a 70-element bismuth germanate ball. In the second experiment a 125-MeV ^{28}Si beam was used and 2.5×10^9 particle-γ-γ-γ and higher-fold coincidence events were detected with the Microball [10], a 95-element CsI(Tl) charged-particle detector array, and the Gammasphere array [11] comprising 83 Compton-suppressed Ge detectors (with the collimators removed to allow γ-ray multiplicity and sum-energy measurements [12]). The $\alpha 2p$ evaporation channel leading to ^{62}Zn represented $\sim$16% (10%) of the total fusion cross section at the lower (higher) bombarding energy, and was selected cleanly in each case by applying the total energy plane channel-selection method [13] to events in which an alpha particle and two protons were detected.

Two sets of strongly coupled bands were observed in ^{62}Zn in the first experiment. The higher beam energy, greater statistics, and improved efficiency for high-energy γ rays in the second experiment enabled the extension of these bands to higher spin and the observation of transitions linking them to the decay scheme. Figure 1 shows a partial level scheme for ^{62}Zn. Spin assignments are based on directional correlations from oriented states. Many of

 0031-9007/98/80(12)/2558(4)$15.00

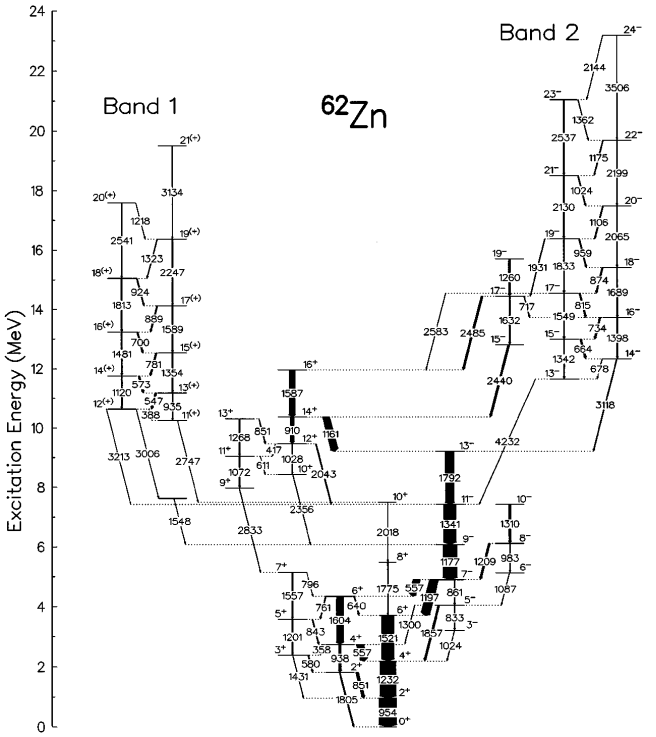

FIG. 1. Partial level scheme of ^{62}Zn. Transition energies are given to the nearest keV.

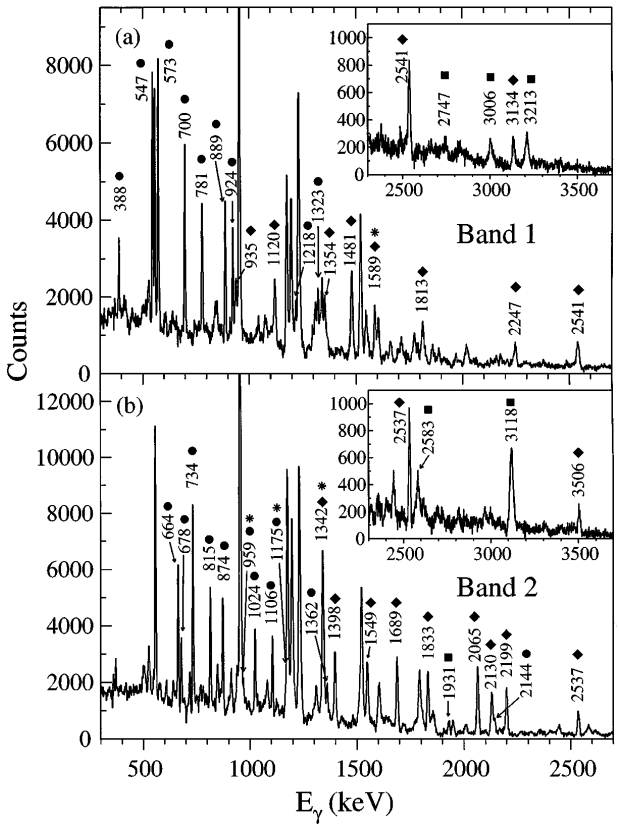

FIG. 2. γ-ray spectra generated by summing spectra in coincidence with the transitions in (a) band 1 and (b) band 2. Symbols denote $E2$ (diamonds) and $M1$ (circles) band members, and transitions (squares) linking the bands to the rest of the decay scheme. Asterisks mark strongly contaminated transitions whose spectra were not included in the sum.

the levels up to the 11^- state were previously known [14,15]. Here we focus on the strongly coupled bands. Figure 2 shows γ-ray spectra obtained by summing coincidence gates set on members of these bands.

To assign configurations to these bands we have used the configuration-dependent shell-correction approach [16,17] with the cranked Nilsson potential (parameters from Ref. [16]) to analyze high-spin states in ^{62}Zn. The calculated energies of favored configurations are compared with the experimental data in Fig. 3. We note how the maximum attainable spin increases with single-particle excitations; $I^\pi_{\max} = 10^+$ with all of the valence particles in $(f_{5/2}p_{3/2})$, 13^- with a neutron excited to $g_{9/2}$, 16^+ with also a proton excited to $g_{9/2}$, 19^- if another neutron is excited to $g_{9/2}$ or 21^+ if a proton hole is made in $f_{7/2}$, and finally, before superdeformed (SD) bands become favored, 24^- with both the latter excitations. All of the corresponding bands have their counterparts in the experimental spectrum. Of special interest are the last two configurations mentioned above which have a single proton hole in the $f_{7/2}$ shell. These configurations lead to strongly coupled rotational bands with large $M1$, as well as $E2$, transition probabilities. Based on the excellent agreement between the calculations and experiment, we assign these configurations ([11,01] and [11,02] in the notation of Fig. 3) to the observed bands 1 and 2.

Bands 1 and 2 in ^{62}Zn are examples of smoothly terminating bands which are observed over extended spin ranges up to their terminating states. As shown in Fig. 4, these bands are calculated to be triaxial at intermediate spins and to change shape gradually, terminating in noncollective oblate ($\gamma = 60°$) states. We note that, unlike the bands in the $A \sim 110$ mass region which are predicted to lose quadrupole deformation as they approach termination [17], these bands in ^{62}Zn are calculated to remain well deformed ($\varepsilon_2 \sim 0.23 - 0.29$) over their entire spin range. The transition to an oblate state nevertheless implies a loss of collectivity, and hence decreasing transition quadrupole moments. Despite the predicted loss of collectivity, the high transition energies in these bands lead to short lifetimes, and they are observed to decay almost entirely while the recoiling nuclei are slowing down in the thin target. Transition quadrupole moment Q_t measurements for these bands can thus be made by the thin target Doppler shift attenuation method [18]. Figure 5 shows the measured fraction F of the full Doppler shift for transitions in these bands.

In order to extract Q_t values from these measurements the slowing down of the recoiling nuclei in the target was modeled with the electronic stopping powers of Northcliffe and Schilling [19] scaled by the Ziegler and Chu [20] stopping powers for ^{4}He as suggested by Sie *et al.* [21]. The decay of the strongly coupled bands was modeled with the experimental transition energies and $E2/M1$ branching

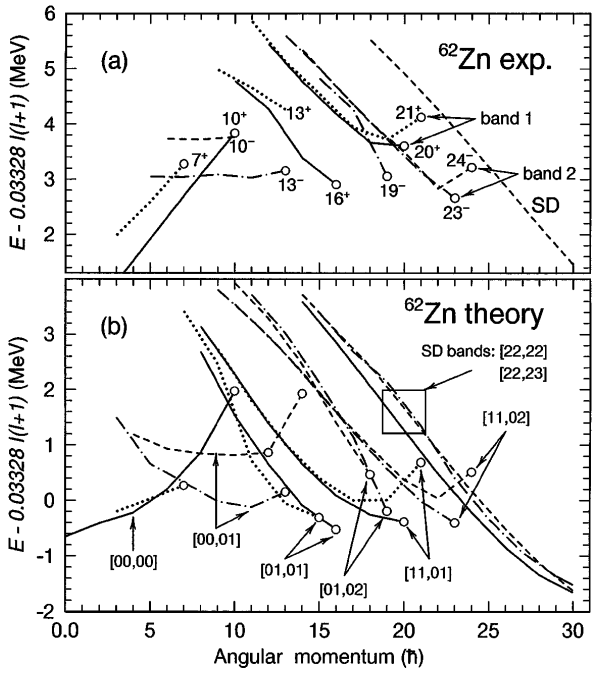

FIG. 3. Energies of states in ^{62}Zn relative to an $I(I+1)$ reference from (a) experiment and (b) theory. The parity π and signature α of each configuration is given by the line type: $(\pi,\alpha) = (+,0)$, solid line; $(+,1)$, dotted line; $(-,0)$, dashed line; and $(-,1)$, dot-dashed line. Terminating states are shown by open circles. The highest spin state observed in each configuration is labeled in (a). In (b) the shorthand configuration notation $[p_1p_2,n_1n_2]$ is used where p_1 (n_1) is the number of proton (neutron) $f_{7/2}$ holes, p_2 (n_2) is the number of proton (neutron) $g_{9/2}$ particles, and the ^{62}Zn ground-state valence configuration is $[00,00] \equiv \pi[f_{5/2}p_{3/2}]^2 \otimes \nu[f_{5/2}p_{3/2}]^4$.

ratios, and the unobserved side feeding into each state was modeled by a single transition with $Q_t = 1.0\ e$ b, an energy 0.5 MeV greater than the subsequent in-band transition, and an intensity to match the measured intensity profile. The consequences of this assumed side-feeding structure will be discussed below. Best fits to the low-spin members of bands 1 and 2 under the assumption of constant in-band Q_t values are shown by the dot-dashed lines in Figs. 5(a) ($Q_t = 0.80\ e$ b) and 5(b) ($Q_t = 1.12\ e$ b), respectively. These fits clearly predict F values at the tops of the bands which are greater than the measured values. We note that the value for the unattenuated recoil velocity entering into these measurements is confirmed by the measured F values for the very fast transitions in the ^{62}Zn SD band [22]. To fit all of the experimental data (solid lines in Fig. 5) we have allowed the Q_t values to vary freely within the bands (one free parameter per data point). The derived Q_t values (squares), together with the calculated values (dashed lines), are plotted versus the spin I of the initial state in the insets of Fig. 5. These Q_t values decrease as the terminating states are approached and reach values corresponding to noncollective transition strengths of approximately one Weisskopf unit ($Q_t \sim 0.2\ e$ b) at

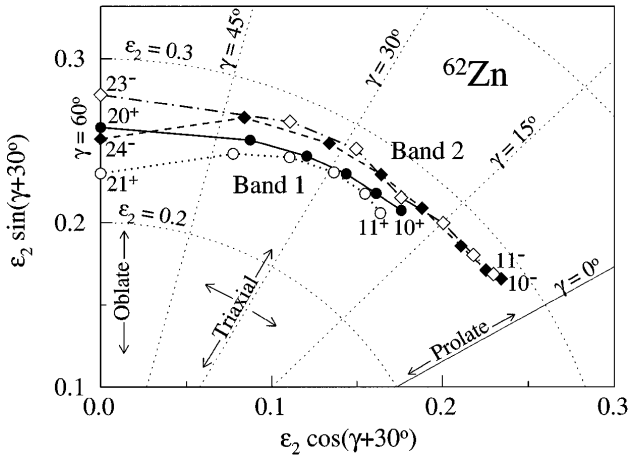

FIG. 4. Calculated shape trajectories in the (ϵ_2,γ) plane for band 1 (circles) and band 2 (diamonds).

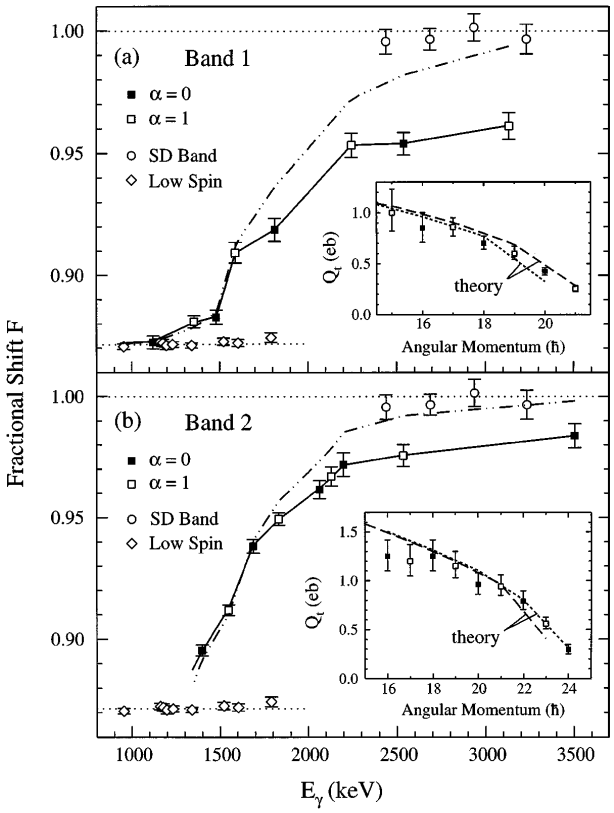

FIG. 5. Fractional Doppler shifts F for transitions in the $\alpha = 0$ (solid squares) and $\alpha = 1$ (open squares) signatures of (a) band 1 and (b) band 2. Also shown are the F values for transitions at the top of the SD band (circles) and from states with $I \leq 13\hbar$ (diamonds). The dotted lines at $F = 1.00$ and 0.872 represent the full shift and the constant shift for decays outside of the thin target, respectively. The dot-dashed lines are fits to the low-spin members of the bands assuming constant in-band Q_t values and the solid lines are fits allowing Q_t to vary freely within the bands. The Q_t values extracted from the latter fits are plotted versus the spin of the initial state in the insets. The short (long) dashed lines in these insets show the calculated Q_t values for the $\alpha = 0$ ($\alpha = 1$) signatures.

the highest angular momenta. The calculated Q_t for the $I \rightarrow I - 2$ transition has been taken as the average of the Q_t values calculated (as described in Ref. [23]) for the I and $I - 2$ states. Although these calculations do not account for the imperfect overlap of the shape wave functions for the initial and final states, and should thus be treated with caution close to termination where the shape change per transition is large [17], the general decreases in Q_t which they predict are in excellent agreement with experiment.

The side-feeding model discussed above is similar in form to that found appropriate in the feeding of SD bands [24], and was chosen to produce plausible mean time delays associated with the feeding of these bands. There is clearly an uncertainty associated with this model. To investigate the sensitivity of the extracted in-band Q_t values to the side-feeding structure the side-feeding Q_t values and the number of transitions in the side-feeding cascades were varied. For example, increasing the side-feeding times by a factor of 2 leads to increases in the extracted in-band Q_t values not exceeding the error bars shown in Fig. 5 (i.e., the statistical uncertainties). As an alternative test of the model we may assume that the in-band Q_t values remained constant with spin. A fit to the data is then obtained by allowing the side-feeding Q_t to vary independently for each state. The results of such fits are that the side-feeding times must *increase* with increasing spin. The competition between statistical $E1$ and collective $E2$ transitions in the γ decay following a fusion-evaporation reaction [25], however, leads to the general expectation that feeding times become systematically shorter with increasing spin. It is unlikely that this situation would ever be reversed, and therefore we conclude that the in-band Q_t values decrease in these smoothly terminating bands.

In summary, we have observed two sets of smoothly terminating strongly coupled bands in ^{62}Zn. Lifetime measurements indicate that the transition quadrupole moments in these bands decrease as termination is approached. These results establish the first terminating states of rotational bands in the $A \sim 60$ mass region and confirm the predicted loss of collectivity associated with smooth band termination. Further studies of smoothly terminating bands in this mass region will undoubtedly lead to a more detailed understanding of this gradual loss of collectivity. These nuclei are also of particular interest because they lie just at the limits of modern large-scale shell model calculations [7]. Future studies of the transition from collective rotation to noncollective terminating states in these light nuclei should provide unique opportunities to compare the mean-field cranking models of rotational nuclei with the microscopic shell model.

This work has been funded by NSERC (Canada), AECL, the DOE under Contracts No. DE-AC05-96OR22464 and No. DE-AC03-76SF00098 and Grants No. DE-FG05-88ER40406 and No. DE-FG05-93ER40770, BMBF (Germany) under Contracts No. 06-OK-668 and No. 06-LM-868, and SNSRC and RSAS (Sweden).

*Present address: Physics Division, Oak Ridge National Laboratory, Oak Ridge, TN 37831-6371.
†Present address: Nuclear Science Division, Lawrence Berkeley Laboratory, Berkeley, CA 94720.
‡Permanent address: Nuclear Research Center, Latvian Academy of Sciences, LV-2169 Salaspils, Latvia.

[1] I. Ragnarsson *et al.*, Phys. Scr. **34**, 651 (1986).
[2] V. P. Janzen *et al.*, Phys. Rev. Lett. **72**, 1160 (1994).
[3] I. Ragnarsson *et al.*, Phys. Rev. Lett. **74**, 3935 (1995).
[4] V. P. Janzen *et al.*, in Proceedings of the Conference on Nuclear Structure at the Limits, Argonne National Laboratory Report No. ANL/PHY-97/1, 1997, p. 171, and references therein.
[5] I. Ragnarsson and A. V. Afanasjev, in Proceedings of the Conference on Nuclear Structure at the Limits (Ref. 4), p. 184, and references therein.
[6] A. Galindo-Uribarri *et al.* (to be published).
[7] D. J. Dean, in Proceedings of the Conference on Nuclear Structure at the Limits (Ref. 4), p. 232.
[8] A. Galindo-Uribarri, Prog. Part. Nucl. Phys. **28**, 463 (1992).
[9] H. R. Andrews *et al.*, Report No. AECL-8329, 1984.
[10] D. G. Sarantites *et al.*, Nucl. Instrum. Methods Phys. Res., Sect. A **381**, 418 (1996).
[11] I.-Y. Lee, Nucl. Phys. **A520**, 641c (1990).
[12] M. Devlin *et al.*, Nucl. Instrum. Methods Phys. Res., Sect. A **383**, 506 (1996).
[13] C. E. Svensson *et al.*, Nucl. Instrum. Methods Phys. Res., Sect. A **396**, 228 (1997).
[14] L. Mulligan, R. W. Zurmühle, and D. P. Balamuth, Phys. Rev. C **19**, 1295 (1979).
[15] N. J. Ward *et al.*, J. Phys. G **7**, 815 (1981).
[16] T. Bengtsson and I. Ragnarsson, Nucl. Phys. **A436**, 14 (1985).
[17] A. V. Afanasjev and I. Ragnarsson, Nucl. Phys. **A591**, 387 (1995).
[18] B. Cederwall *et al.*, Nucl. Instrum. Methods Phys. Res., Sect. A **354**, 591 (1995).
[19] L. C. Northcliffe and R. F. Schilling, Nucl. Data Tables **A7**, 233 (1970).
[20] J. F. Ziegler and W. K. Chu, At. Data Nucl. Data Tables **13**, 463 (1974).
[21] S. H. Sie *et al.*, Nucl. Phys. **A291**, 443 (1977).
[22] C. E. Svensson *et al.*, Phys. Rev. Lett. **79**, 1233 (1997).
[23] A. V. Afanasjev and I. Ragnarsson, Nucl. Phys. **A608**, 176 (1996).
[24] H. Savajols *et al.*, Phys. Rev. Lett. **76**, 4480 (1996).
[25] T. Døssing and E. Vigezzi, Nucl. Phys. **A587**, 13 (1995).